Impact of multi-focused images on recognition of soft biometric traits

V. Chiesa[a], J.L. Dugelay[a]
[a]EURECOM, Campus SophiaTech, 450 Route des Chappes, CS 50193 - 06904 Biot Sophia Antipolis cedex, FRANCE

ABSTRACT

In video surveillance semantic traits estimation as gender and age has always been debated topic because of the uncontrolled environment: while light or pose variations have been largely studied, defocused images are still rarely investigated. Recently the emergence of new technologies, as plenoptic cameras, yields to deal with these problems analyzing multi-focus images. Thanks to a microlens array arranged between the sensor and the main lens, light field cameras are able to record not only the RGB values but also the information related to the direction of light rays: the additional data make possible rendering the image with different focal plane after the acquisition. For our experiments, we use the GUC Light Field Face Database that includes pictures from the First Generation Lytro camera. Taking advantage of light field images, we explore the influence of defocusing on gender recognition and age estimation problems.
Evaluations are computed on up-to-date and competitive technologies based on deep learning algorithms. After studying the relationship between focus and gender recognition and focus and age estimation, we compare the results obtained by images defocused by Lytro software with images blurred by more standard filters in order to explore the difference between defocusing and blurring effects. In addition we investigate the impact of deblurring on defocused images with the goal to better understand the different impacts of defocusing and standard blurring on gender and age estimation.
.

Keywords: Multi-focused images, gender recognition, age estimation

1. INTRODUCTION

The recognition of hard and soft biometric traits in unconstrained environment is still an open challenge: in videosurveillance light and pose variations and low camera resolution hamper recognition algorithms from having good performance.
Despite having obtained nearly perfect results in the past years on gender recognition on controlled environment [1], the accuracy on more challenging database like Labeled Faced in the Wild is still low: in [2] authors combine LBP and SVM reaching an accuracy of 94.81%. Tapia and Perez [3] succeed to classify the 98% of subjects using the same dataset for training and testing. In [4] authors explore a possible correlation between gender recognition and age but they do not outperform the previous works. One of the most performant algorithm right now in unconstrained database is described in [5]: the method is based on LBP features and C-Pegasos classifier and reaches an accuracy of 96.86%.
While humans can easily recognize gender, age estimation is a hard task not only for automatic algorithms: aging process is different for each person and influenced by environmental factors. Moreover apparent age and biological age often do not coincide: that get more difficult the collection of apparent age database and, thus, of a complete analysis of the problem. In 2015 a dataset of faces labeled with apparent age has been collected in order to conduct the first ChaLearn Looking at People competition and it has been increased in 2016 [6]. The best performance on both biological and apparent age estimation have been achieved with CNN architectures pre-trained and later fine-tuned on the particular problem [7], [8].
Multiple studies have been done in order to better understand the influence of light and pose variation in biometrics: in [9] the authors explore a possible relation between gender recognition and emotion and in [10] an algorithm to estimate age under different light condition is described. In [11] MLBP, Gabor filtering, PCA and SVR are used to describe the age characteristics of motion blurred images. In [12] authors study the influence of privacy filters on automatic gender recognition method and on a crowdsourcing classification proving that the robustness of computer vision and of human classification are close.

Further authors information:
Valeria Chiesa: chiesa@eurecom.fr
Jean-Luc Dugelay: dugelay@eurecom.fr

Although out-of-focus is one crucial factor of image quality degradation, its impact in biometrics has not been largely studied and often it is associate to other kind of blurring processes. In [13], Fang Hua et al. analyze the influence of defocusing on face recognition working on images from Q-FIRE database [14] generated by turning the camera ring and acquiring multiple shots.
The emergence of new technologies as plenoptic cameras yields to deal with defocusing problem with a database generated by single shots. This avoids possible pose or light variations, motion blur or different camera aberrations, yields to concentrate on defocusing problem. Plenoptic images have been rarely used until now in biometrics: in [15] the creation of a light field database for face and iris is described and a first exploration of the usefulness of plenoptic is done. A new method to remove eyelash for iris recognition is investigated in [16] and in [17] authors take advantages of light field technology for face recognition at distance. Anti-spoofing abilities are investigated successfully in [18].
In this paper we want to analyze the impact of multi-focused images on gender recognition and age estimation in order to improve in the future the preprocessing applied on these problems. First we hypothesize and verify the presence of a linear correlation between the focus level of the picture and both the quality of gender recognition and age estimated. Then, we investigate the different behavior of the two classifiers on Gaussian blurred images verifying a strong relation between defocused and blurred images. In order to improve the robustness of our analysis we study the diagnostics of linear regressions with "dummy" variable and the shape of the prevision interval of a linear regression fitted with blurred images. In the last part we explore the impact of deblurring filtering applied on defocused images.

1.1 Light field

Light field cameras have been developed by Lippmann in 1908 and evolved by Adelson and Wang [19]. The operating principle is based on the possibility of describing all light information of a scene in a single function called *Plenoptic function* (1)

$$L = L(\theta, \phi, \lambda, t, V_x, V_y, V_z) \tag{1}$$

Where (θ, ϕ) are the spherical coordinates describing the direction of the light ray, λ the wavelength, t is the time and (V_x, V_y, V_z) are the coordinates of the viewing position. Since we are interested in still images and we consider only 3 different wavelength (RGB), we can represent the plenoptic function as a 5-dimensional function parameterizing a light ray like in (Figure 1). 5-dimentional plenoptic function can be represented also with a different parametrization called light field [20].

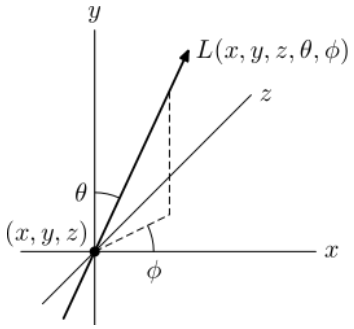

Figure 1: Visual representation of 5-dimentional plenoptic function [21]

With plenoptic function is possible to describe completely a 3-dimentional space illuminated by multi-chrome light at each moment. Thanks to this principle, in 2006 Ren Ng works on hand held plenoptic camera [22] and in 2011 the first commercial plenoptic cameras appear on the market with the brand Raytrix and Lytro. From a mechanical point of view the principal difference between standard and light field cameras is the presence of a microlenses array between the main lens and the sensor. In this condition, multiple images from difference angulation are saved on the sensor and with post processing operations it is possible to reconstruct the complete light field information.
With plenoptic camera, thus, we are able to adjust the focus of an image, within a large range of values, after the acquisition. The number of possible focus plane is dependent on the camera setting at the moment of the acquisition.

2. EXPERIMENT

2.1 Database

Our analysis have been done on the GUCLF Light Field Face Database from NUTU [15]. This database is composed by 102 subjects, 70 male and 32 female, aging from 18 to 65 years and different ethnicities.
The database is divided in two main parts. In the first part 8 high resolution images for each subject with different poses and expressions are collected. The acquisition has been done in a controlled environment, with uniform illumination and without shadows cast on faces. In order to respect the ICAO guidelines, the authors employed a Canon EOS 550D DSLR camera. The second part consists in bmp format images obtained by processing the light field data acquired with a commercial First Generation Lytro camera. Light field images represent multiple subjects at different distance from the camera in the same picture and they have been collected following three different protocols: indoor with only artificial light, indoor with both sunlight and artificial light and outdoor with sunlight. The post process applied on the database by authors consists in saving each image in a bmp format changing focus level thanks to Lytro Software. Then faces present in each picture have been detected, cropped and resized to 120x120 pixels in grayscale bmp format. The images available in the database, therefore, are around 2980 in total and show faces present multiple times with different focus levels (Figure 2). Background is almost negligible and, because faces have been cropped, it is not possible to define which persons are present in the same image. We do not have access to metadata as gender or age. Gender has been hand annotated by us looking at the standard images, for age has been preferred to analyze the behavior respect to the focus without investigate the accuracy of the classifier.
The post process operated by the authors on light field images limits our work but as far as we know this is the only biometric light field database available.

Figure 2: Different focus levels for the same picture

2.2 Gender recognition from face

Since the GUCLF Light Field Face Database is composed of pictures collected in unconstrained environment, for gender recognition we choose to use an algorithm with strong performance on challenge cross-dataset protocols. For this reason we use the minimalistic CNN-based ensemble model described in [23]. The classifier has as input an aligned face and returns a real value between 0 and 1. That value indicates the probability for the subject of being female.

2.3 Age estimation from face

In order to estimate age from face we use the winner algorithm of 2016 ChaLearn LAP competition on Apparent Age Estimation [24]. The work is based on a VGG-16 convolutional neural network pre-trained for face recognition, trained on IMDB-Wiki dataset and fine-tuned using the competition dataset. Although the strong point of the method is apparent age estimation on children, this algorithm is one of the most performant on adults too.

2.4 Preprocessing

In a first analysis we find out that the accuracy of gender classifier on standard images is of 99.61% and of 95.25% on images extracted from the light field camera.

With the aim to study the impact of defocusing on gender recognition and age estimation we set a metric able to describe the picture quality. We use the Modular Transfer Function (MTF), a metric often used to evaluate image quality [13]: it is defined as the magnitude of Optical Transfert Function and can be calculate as (2):

$$MTF = \sum_{n=0}^{N-1} y_n e^{-ikn\frac{2\pi}{N}} \tag{2}$$

Where $k \in [0, N-1]$ and y_n is the position of the n^{th} pixel.
In order to find a relation between MTF and the score obtained as output of the CNN, the same picture at different focus levels has been analyzed. We find a linear correlation between these values. In (Figure **3**) is shown an example of how defocusing influences the classifier output: the more the MTF increases, the more the score approaches the 0 value and in this case the correct classification because the person present in the image is a man.
In a parallel way we study how age estimation changes with MTF variation. Here we are interested only on the trend of apparent age compare to MTF and real age is not a fundamental information. We follow the same procedure described in the previous paragraph to analyze the output of the age estimator. In (Figure 4) is possible to notice the linear correlation between age estimated and MTF.

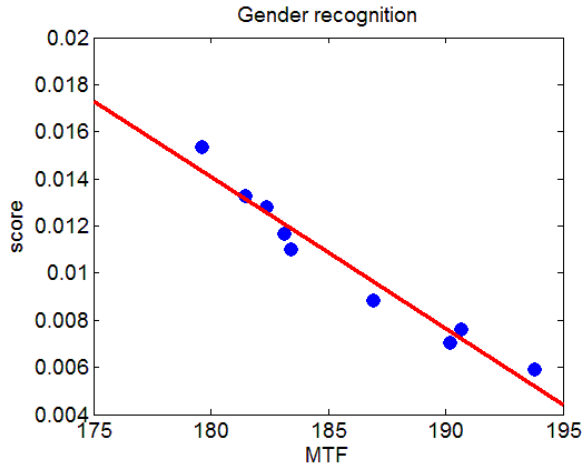

Figure 3: Example of linear relation between gender score and MTF

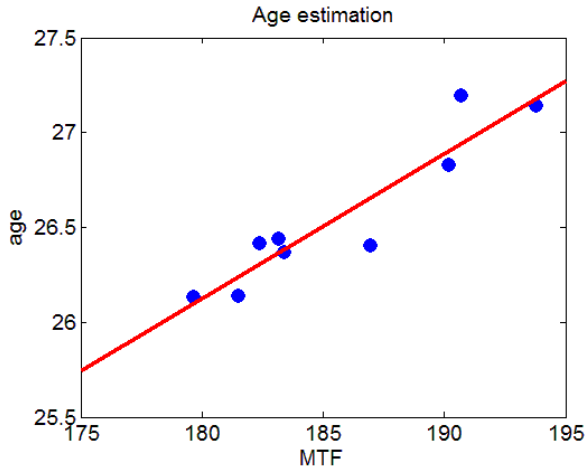

Figure 4: Example of linear relation between age estimated and MTF

2.5 Experiment I

The first experiment consists in verifying if the correlation between gender score and MTF is linear for all pictures. It is important to highlight that the purpose of this experiment is not to find a function describing the general relation between defocusing and gender score because the huge influence of image content would make it hard. With the aim to analyze each set of defocused pictures separately, we select the images where are present four or more versions with different focus levels. For each set we compute 2 models of linear regression where the dependent variable (y) is the gender score and the independent variable (x) is the MTF.

$$\text{Model 1:} \quad y \sim \beta_0 + \beta_1 x \tag{3}$$

$$\text{Model 2:} \quad y \sim \beta_0 + \beta_1 x + \beta_2 x^2 \tag{4}$$

For each model we study the distribution of the R^2 value. A perfect representation of the model would present a delta distribution in the 1 value: the high asymmetry of the histograms suggests that model 2 fits better on the data (Figure 5, Figure 6), but we are inclined to choose the first model and to keep as low as possible the number of regressors because of the lack of samples.

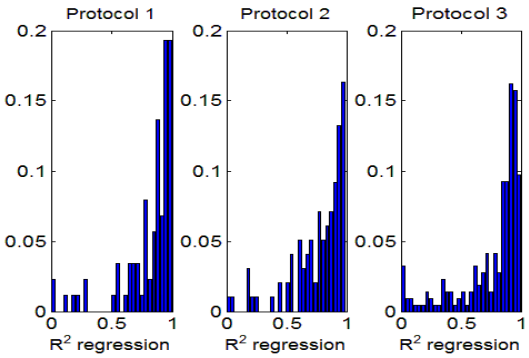

Figure 5: Histograms of R^2 of Model 1 for gender recognition

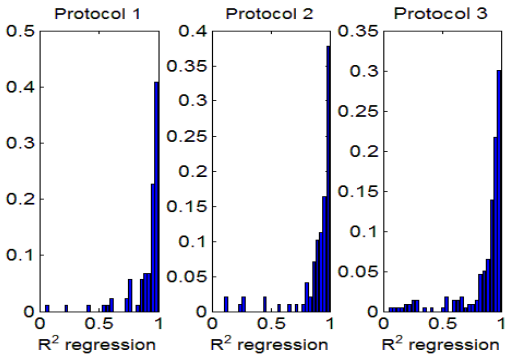

Figure 6: Histogram of R^2 of Model 2 for gender recognition

For the second part of the first experiment we follow the same procedure described for gender recognition, but as independent variable we use the age estimated. While in the gender recognition case the protocol used in images collection has not a particular influence, here the different light condition changes critically the results (Figure 7). However we notice that the angular coefficient of the regression line in protocol 1 and 2 is always positive and in protocol 3 only the 6,98% of the cases have negative coefficients. The fact that the sharper the image is, the older the person looks like is not surprising: age markers (like skin spot or wrinkles) are mostly stored in high frequencies and become less visible when the picture is out-of-focus. The particular behavior observed on protocol 3 could be explained considering the more challenge environment: on one hand, light variations during the acquisition process have almost no influence on gender recognition, on the other hand, age estimation seems to be strongly influenced by environment variations.

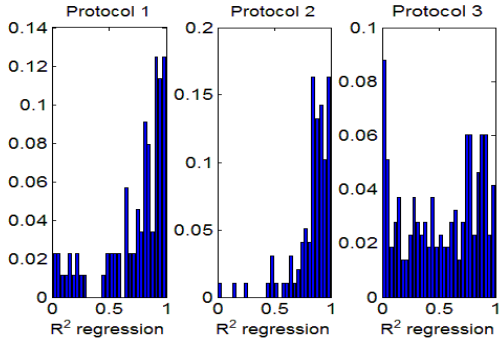

Figure 7: Histograms of R^2 of Model 1 for age estimation

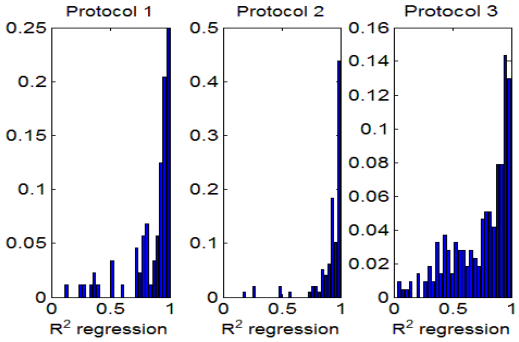

Figure 8: Histograms of R^2 of Model 2 for age estimation

2.6 Experiment II

Part a

In human vision, defocusing and Gaussian blurring are really similar although the generation processes are different. The second experiment has been done with the purpose of studying the possible difference between the influence of defocusing and Gaussian blurring on soft biometric traits. For each image we choose the "most on focus" version and a we apply seven Gaussian filters with dimension between 3x3 pixels and 15x15 pixels. We analyze as described in experiment I the blurred images and we find out that the linear behavior is confirmed for all protocols with the exception of protocol 3 for age estimation.

In order to compare the relation between gender score and MTF on defocused images and gender score and MTF on blurred images we evaluate different regression models for each set of picture, considering both the defocused and the blurred versions. We fit four different models where the dependent variable (y) is the gender score, the independent variable (x) is the MTF value and the dummy variable (d) has value 1 for the blurred images and 0 for the defocused images. A high p-value for the coefficients relate to dummy variables indicates that they are not statistically significant and, thus, that differences between the defocused and blurred images are not statistically significant.

$$\text{Model 1} \qquad \boldsymbol{y \sim \beta_0 + \beta_1 d + \beta_2 x + \beta_3 xd} \tag{5}$$

$$\text{Model 2} \qquad \boldsymbol{y \sim \beta_0 + \beta_1 d + \beta_2 x} \tag{6}$$

$$\text{Model 3} \qquad \boldsymbol{y \sim \beta_0 + \beta_1 d} \tag{7}$$

$$\text{Model 4} \qquad \boldsymbol{y \sim \beta_0 + \beta_1 x} \tag{8}$$

The results show how, for all protocols, in the first model, although the percentage of high correlation coefficient is close to 87%, the two regressors related to the dummy variable have more likely coefficients with value equal to 0. In the second model the percentage related to R^2 is inferior to model 1 and again the dummy variable seems to be superfluous. The third model represents two horizontal regression lines and clearly it doesn't fit our data. The last model suggests that both defocusing and blurring influence on the same way the gender recognition classifier.

	$R^2 > 0.7$	$P-value < 0.2$ β_0	$P-value < 0.2$ β_1	$P-value < 0.2$ β_2	$P-value < 0.2$ β_3
Model 1	86.36	78.78	37.87	74.24	36.36
Model 2	80.30	100	43.93	98.48	/
Model 3	0	75.75	42.42	/	/
Model 4	**71.21**	**100**	**98.48**	/	/

Table 1: Protocol 1, gender recognition: percentage of $\boldsymbol{R^2}$ superior of 0.7 and percentage of low p-value for coefficient evaluated for each Model

	$R^2 > 0.7$	$P-value < 0.2$ β_0	$P-value < 0.2$ β_1	$P-value < 0.2$ β_2	$P-value < 0.2$ β_3
Model 1	85.71	79.76	38.09	78.57	30.95
Model 2	72.61	97.61	21.42	97.61	/
Model 3	0	76.19	33.33	/	/
Model 4	**65.47**	**97.61**	**98.80**	/	/

Table 2: Protocol 2, gender recognition: percentage of $\boldsymbol{R^2}$ superior of 0.7 and percentage of low p-value for coefficient evaluated for each Model

	$R^2 > 0.7$	$P-value < 0.2$ β_0	$P-value < 0.2$ β_1	$P-value < 0.2$ β_2	$P-value < 0.2$ β_3
Model 1	83.74	81.77	50.73	85.22	48.27
Model 2	71.92	95.07	50.24	95.07	/
Model 3	0	90.14	42.85	/	/
Model 4	**56.65**	**92.61**	**94.58**	/	/

Table 3: Protocol 3, gender recognition: percentage of $\boldsymbol{R^2}$ superior of 0.7 and percentage of low p-value for coefficient evaluated for each Model

The same procedure described above for gender recognition has been applied on age estimation. Also in this case we can say that blurred and defocused images have the same regression line. Despite the fact that the percentage of P-value related to coefficients of dummy variables lower than 0.2 is higher than in the previous case, the model described in (8)

can still be considered the best. In the third protocol the percentage of high correlation is lower than 40% for the fourth model: that is due to the instability of age estimation algorithm on different light conditions.

	$R^2 > 0.7$	$P-value < 0.2$ β_0	$P-value < 0.2$ β_1	$P-value < 0.2$ β_2	$P-value < 0.2$ β_3
Model 1	87.87	59.09	42.42	68.18	36.36
Model 2	81.81	84.84	40.90	98.48	/
Model 3	01.51	100	54.54	/	/
Model 4	**74.24**	**78.78**	**98.48**	/	/

Table 4: Protocol 1, age estimation: percentage of $\boldsymbol{R^2}$ superior of 0.7 and percentage of low p-value for coefficient evaluated for each Model

	$R^2 > 0.7$	$P-value < 0.2$ β_0	$P-value < 0.2$ β_1	$P-value < 0.2$ β_2	$P-value < 0.2$ β_3
Model 1	95.23	54.76	47.61	84.52	41.66
Model 2	86.90	65.47	35.71	1	/
Model 3	0	100	29.76	/	/
Model 4	**80.95**	**66.66**	**98.80**	/	/

Table 5: Protocol 2, age estimation: percentage of $\boldsymbol{R^2}$ superior of 0.7 and percentage of low p-value for coefficient evaluated for each Model

	$R^2 > 0.7$	$P-value < 0.2$ β_0	$P-value < 0.2$ β_1	$P-value < 0.2$ β_2	$P-value < 0.2$ β_3
Model 1	**63.05**	**75.86**	**50.24**	**70.93**	**46.79**
Model 2	44.82	84.23	47.78	85.71	/
Model 3	0	100	34.97	/	/
Model 4	34.97	84.72	84.72	/	/

Table 6: Protocol 3, age estimation: percentage of $\boldsymbol{R^2}$ superior of 0.7 and percentage of low p-value for coefficient evaluated for each Model

Part b

In order to confirm the hypothesis that the influence of Gaussian blurring and defocusing is the same on gender recognition and age estimation we fit linear regressions based only on blurred images and we check which percentage of defocused images fall in the prevision interval of the regression. We choose to use a confidence of 95% in the prevision intervals computation. Results show how the 89% of defocused images have more than 80% of their versions in the prevision interval in protocol 1. The behavior of defocused pictures and the blurred ones is less similar if the environment is unconstrained.

The same experiment on age estimation has coherent results regards to the previous analysis: while we can accept the hypothesis of same influence for the first two protocols, the last one presents values particularly low.

	Gender recognition problem (> 80%)	Age estimation problem (> 80%)	Gender recognition problem (> 50%)	Age estimation problem (> 50%)
Protocol 1	**89.39**	**80.30**	95.45	95.45
Protocol 2	84.34	75.90	95.18	87.95
Protocol 3	60.10	51.23	86.70	72.91

Table 7: Percentage of images of which at least of 80% and 50% of defocused versions are present in the prevision interval

2.7 Experiment III

As last experiment we analyse the influence on soft biometric traits of a deblurring filter applied on defocus images. For each image, for each defocus version, we look for the most similar, in terms of MTF, blurring version of the same image. Knowing the window size of the convolution done to blur the image, we can guess the best deconvolution window for the defocus picture. As deblurring filter we use a blind deconvolution algorithm based on a convolution between image and Point Spread Function (PSF): the method looks for the best PSF so that the resulting image has the higher probability of being an instance of the blurred image, with the assumption of Poisson noise statistics. Blind deconvolution can be used when no information about distortion is available, like in the case of defocused pictures.

While the impact of deblurring filter on blurred images is always positive and increase the MTF, only for a relatively small percentage of defocused images, it is effective as show in (Table 8) . The higher percentage of improvement in protocol 3 is due to the lower quality of the images, strongly influenced by the environment.

	Defocused images	Blurred images
Protocol 1	55.77	100
Protocol 2	66.66	100
Protocol 3	**70.77**	100

Table 8: Percentage of images where the MTF increase after deblurring filter application

In (Table 9) the percentage of improvement on gender recognition and age estimation is shown. As improvement for gender recognition we consider a lower error respect to the ground truth, for age estimation we consider the increasing of age estimated. As we expect, classification on defocused images is less subject to deblurring filter than classification on blurred images. Moreover, gender recognition appears more impacted by deblurring respect to age estimation, possibly because of artifacts created by deblurring algorithm.

	Gender recognition defocused images	Gender recognition blurred images	Age estimation defocused images	Age estimation blurred images
Protocol 1	61.55	78.73	39.11	62.33
Protocol 2	**68.38**	81.00	47.42	67.89
Protocol 3	67.77	**82.60**	**64.84**	**71.29**

Table 9: Percentage of images where deblurring improved the recognition of soft biometric traits

3. CONCLUSION

In this work we demonstrate the linear relation between focus and gender recognition in a database acquired with a plenoptic camera: we find out that the sharper an image is, the more accurate the classifier is. We test our hypothesis on different environments and, although in a sunlight condition the linearity is less obvious, we confirm the presence of a linear model. We redo the same analysis for age estimation and we discover that linearity is preserved only with artificial or semi artificial light. Moreover there is a strong evidence that the sharper the image is, the higher the apparent age is: this is not surprising if we consider that age signs, as wrinkles and skin spots, are mainly present in high frequencies.
Then, we compare defocused and blurred images in order to propose a unified model. Both the regression with dummy variable and the study of prevision interval confirm that we can assume the same behavior for defocused and blurred images on gender recognition problem. Age estimation classifier looks more influenced by light variation and we cannot assert that blurred and defocused images share the same model in the condition presented in protocol 3.

We investigate the impact of a deblurring filter on defocused images finding that are less subject to deblurring than the blurred images. Then, we compare the improvement generated by the blind deconvolution on gender recognition and age estimation and we observe that gender recognition appears to be more influenced by quality of the image.
The analysis presented in this paper are going to be improved as soon as we can access to different light field face database.

4. REFERENCES

[1] M. H. Ihsan Ullah, G. Muhammad, H. Aboalsamh, G. Bebis and A. M. Mirza, "Gender recognition from face images with local WLD descriptor," in *2012 19th International Conference on Systems, Signals and Image Processing (IWSSIP)*, Vienna, 11-13 April 2012.

[2] C. Shan, "Learning local binary patterns for gender classification on real-world face images," *Pattern recognition letters*, vol. 33, pp. 431-437, 2012.

[3] J. E. Tapia and C. A. Perez, "Gender Classification Based on Fusion of Different Spatial Scale Features Selected by Mutual Information," in *IEEE transactions on information forensics and security*, March 2013.

[4] J. Bekios-Calfa, J. M. Buenaposada and L. Baumela, "Robust gender recognition by exploiting facial attributes dependencies," *Pattern recognition letters*, vol. 36, pp. 228-234, January, 2014.

[5] S. Jia and N. Cristianini, "Learning to classify gender from four million images," *Pattern recognition letters*, vol. 58, pp. 35-41, June, 2015.

[6] S. Escalera, M. Torres, B. Martinez, X. Baro, H. J. Escalante and e. al, "Chalearn looking at people and faces of the world: Face analysis workshop and challenge 2016," in *Computer Vision and Pattern Recognition Workshop*, 2016.

[7] R. Rothe, R. Timofte and L. V. Gool, "Deep expectation of apparent age from a single image," in *International conference on Computer Vision Workshop*, 2015.

[8] H.-F. Yang, L. B-Y, C. K-Y and C. C-S, "Automatic age estimation from face images via deep ranking," in *British Machine Vision Conference*, 2015.

[9] K. Zibrek, L. Hoyet, K. Ruhland and R. McDonnell, "Evaluating the effect of emotion on gender recognition in virtual humans," in *ACM Symposium on Applied Perception*, New York, USA, 2013.

[10] K. Ueki, M. Sugiyama and Y. Ihara, "Perceived Age Estimation under Lighting Condition Change by Covariate Shift Adaptation," in *Perceived Age Estimation under Lighting Condition Change by Covariate Shift Adaptation*, 2010.

[11] S. R. C. T. D. P. K. R. P. Dat Tien Nguyen, "Human Age Estimation Method Robust to Camera Sensor and/or Face Movement," *Sensors*, vol. 15, September 2015.

[12] N. Ruchaud, G. Antipov, P. Korshunov, J.-L. Dugelay, T. Ebrahimi and S.-A. Berrani, "The impact of privacy protection filters on gender recognition," in *OPTICS + PHOTONICS 2015, SPIE Optical Engineering + Applications, Applications of Digital Image Processing XXXVIII*, San Diego, USA, 10-13 August, 2015.

[13] F. Hua, P. Johnson, N. Sazonova and S. Schuckers, "Impact of out-of-focus blur on face recognition performance based on modular transfer function," in *5th IAPR International Conference on Biometrics*, New Delhi, March 2012.

[14] P. L.-M. N. S. F. H. S. S. P. A. Johnson, "Quality in face and iris research ensemble (Q-FIRE)," in *Fourth IEEE International Conference on Biometrics: Theory Applications and Systems*, 2010.

[15] R. Raghavendra, K. B. Raja and C. Busch, "Exploring the Usefulness of Light Field Cameras for Biometrics: An Empirical Study on Face and Iris Recognition," in *IEEE Transactions on Information Forensics and Security*, 2016.

[16] G. H. Z. S. Shu Zhang, "Eyelash Removal Using Light Field Camera for Iris Recognition," in *Biometric Recognition* , Springer International Publishing, 2014, pp. 319-327.

[17] R. Raghavendra, K. B. Raja, B. Yang and C. Busch, "Improved face recognition at a distance using light field camera & super resolution schemes," in *6th International Conference on Security of Information and Networks*, November 2013.

[18] S. Kim, Y. Ban and S. Lee, "Face Liveness Detection Using a Light Field Camera," in *Sensors*, December 2014.

[19] W. J. Adelson E., "Single lens stereo with a plenoptic camera," in *IEEE Trans. Pattern Anal. Mach. Intell.*, 1992.

[20] M. Levoy and P. Hanrahan, "Light Field Rendering," in *Proc. ACM Siggraph*, 1996.

[21] "Wikipedia," [Online]. Available: https://en.wikipedia.org/wiki/Light_field.

[22] R. Ng, "DIGITAL LIGHT FIELD PHOTOGRAPHY," PhD Thesis, 2006.

[23] G. Antipov, S.-A. Berrani and J.-L. Dugelay, "Minimalistic CNN-based ensemble model for gender prediction from face images," *Pattern recognition letters*, vol. 70, January 2016.

[24] G. Antipov, M. Baccouche, S.-A. Berrani and J.-L. Dugelay, "Apparent age estimation from face images combining general and children-specialized deep learning models," in *29th IEEE Conference on Computer Vision and Pattern Recognition Workshops*, Las Vegas, USA, 2016.